

Longitudinal- e^- -beam-polarization asymmetry in $e^+e^- \rightarrow$ hadrons

Bryan W. Lynn

Institute for Theoretical Physics, Department of Physics, Stanford University, Stanford, California 94305

Claudio Verzegnassi

*Theoretical Physics Department, University of Trieste, Istituto Nazionale di Fisica Nucleare,
Sezione di Trieste and ISAS (Trieste), Trieste, Italy 34100*

(Received 10 November 1986; revised manuscript received 25 February 1987)

We introduce and analyze the longitudinal-polarization asymmetry of the process $e^+e^- \rightarrow$ hadrons with longitudinally polarized electron beams on and near the Z^0 resonance. We show that, in spite of the intrinsic strong-interaction presence in the final state, the vast majority of the diagrams which contribute to one electroweak loop are free of strong-interaction effects. Further, on Z^0 resonance the asymmetry is independent of the final states, giving a commensurate increase in statistics. We show that for these reasons the total theoretical strong-interaction uncertainty on Z^0 resonance is $\Delta A_{LR}^{e^+e^- \rightarrow \text{hadrons}} \lesssim 0.004$, allowing a measurement of A_{LR} to ± 0.015 (which can be interpreted as a measurement of $\sin^2\theta_W$ to ± 0.002) with only $\sim 5 \times 10^4 Z^0$'s. Further, a measurement of A_{LR} to ± 0.008 , or $\sin^2\theta_W$ to ± 0.001 , can be done with $\sim 10^6 Z^0$'s. This rather peculiar property of the asymmetry could allow Stanford Linear Collider and CERN LEP experiments to test the standard Glashow-Salam-Weinberg (GSW) theory and possible new physics beyond GSW early in the lifetime of these accelerators.

I. INTRODUCTION

In the next few years, a number of high-precision experiments will be carried out which will test electroweak theories at the one-loop level in analogy with experiments which, years ago, probed QED. These include neutrino-electron scattering by the CHARM II Collaboration and CERN LEP and Stanford Linear Collider (SLC) measurements of e^+e^- annihilation.

In this paper we shall focus our attention on the peculiar properties of one specific experiment which will be performed in the near future at SLC (and, perhaps, at LEP) and which, we believe, deserves some rather special treatment: the measurement of the longitudinal-polarization asymmetry in the collision of an unpolarized positron with a longitudinally polarized electron on and near the Z^0 resonance. This process has already been discussed in detail in the case of production of a final $\mu^+\mu^-$ pair and it has been shown¹ that it can represent a very precise test of both the Glashow-Salam-Weinberg (GSW) electroweak theory² at the one-loop level and of possible new physics beyond the GSW theory. This is because radiative corrections to one loop are particularly sensitive to the existence of new heavy particles (in the 100–1000-GeV range) which do not decouple and/or of new gauge bosons—such as a new heavy Z' in the 300–1000-GeV region,³ with substantial mixing with Z^0 . (The same tests could be achieved by measuring the τ polarization in the process $e^+e^- \rightarrow \tau^+\tau^-$, e.g., at LEP.)

One problem with this elegant program is statistics. Roughly $\sim 10^6 Z^0$'s must be produced to achieve a $\sim 1\%$ experimental accuracy corresponding to $\sim 3 \times 10^4 \mu^+\mu^-$ pairs, a luminosity available only at mature SLC or LEP

measurements.

An obvious solution to this problem would be to use final-state hadrons with a commensurate increase in the statistics factor of around 30. The price to pay is that final-state strong interactions introduce uncertainties in the theoretical predictions. We show below though that $A_{LR}^{e^+e^- \rightarrow \text{hadrons}}$ is to high accuracy quite insensitive to strong interactions. Their effects are canceled out by the special properties of the longitudinal-polarization asymmetry. This is in contradistinction to other possible asymmetries with final hadrons such as forward/backward and transverse asymmetries A_{FB} and A_{\perp} , where not only are the strong-interaction effects not canceled, but the difficulties in the precise definition of jet axes make precise definitions of such asymmetries less clear.⁴ Specifically, we will show that to lowest order in α_{em} , $A_{LR}^{e^+e^- \rightarrow \text{hadrons}}$ on Z^0 resonance is not only independent of the identity of the final states but is also unaffected by strong interactions. This is true whether or not one uses perturbative QCD. Thus, the subsequent hadronization of the final-state quarks (liable to be a major source of strong-interaction uncertainty for other experiments) does not affect A_{LR} on resonance.

Off Z^0 resonance, the asymmetry becomes weak-flavor dependent. However, assuming that perturbative QCD can be used, as, e.g., with $uds\bar{c}\bar{b}$ quarks, A_{LR} is still independent of strong interactions, at least through order α_s . This means that off-resonance (only) top-quark production has to be studied separately.

Including electroweak corrections to one loop, the situation described above remains substantially unchanged for the vast majority of such contributions, particularly on Z^0 resonance. We show this below and isolate those dia-

defined by the e^- beam direction for left-handed and right-handed initial-state electrons.

There is a very simple heuristic argument for the independence of $A_{LR}^{e^+e^- \rightarrow \text{hadrons}}$ on Z^0 resonance of the details of the final states. We produce Z^0 's with e_L^- at some rate and they decay. We then produce Z^0 's with e_R^- at a *different* rate and they decay. In the ratio A_{LR} , the decay rate of the Z^0 cancels because we have manipulated only the *initial* state.

Strictly speaking, our result Eq. (2.8) is true to the extent to which one can neglect, on Z^0 resonance, contributions not due to pure Z^0 exchange. Although one knows such terms to be suppressed by small $\sim \Gamma_Z^2/M_Z^2$ factors, their effect has to be studied if one aims to achieve a theoretical prediction at the level of 1% accuracy. This has been thoroughly done, to lowest order in α_{em} , in a previous paper,⁵ and we shall summarize the technique in the Appendix. The result is that the remaining photon-exchange contributions can be safely neglected to 2% accuracy, thus allowing the conclusion of Eq. (2.8) to remain valid within this approximation.

III. A_{LR} OFF RESONANCE TO LOWEST ORDER IN α_{em}

We now examine $A_{LR}^{e^+e^- \rightarrow \text{hadrons}}$ off resonance to lowest order in α_{em} . It is convenient⁴ to write the differential cross section for $e^+e^- \rightarrow \text{hadrons}$ in terms of the inclusive structure functions $W_{1,2,3}^{\alpha\beta}$, where $W_1^{\gamma\gamma}$ comes from the square of the photon exchange, $W_2^{\gamma Z}$ from the square of the Z^0 exchange, and $W_3^{\gamma Z}$ from the interference term between the photon exchange and Z^0 exchange. The inclusive structure functions describe the process $e^+e^- \rightarrow X + \text{anything}$, where X with momentum \vec{p}_μ is some experimentally tagged particle which makes an angle ξ with respect to the electron beam and carries an energy fraction $x = 2\vec{p}_0/\sqrt{s}$ (see Fig. 3). The $W_i^{\alpha\beta}$ are certain functions of x and s . If we generalize the helicity coupling constants g_{Le}, g_{Re} defined in Fig. 1 to include $g_{Le}^\alpha, g_{Re}^\alpha$ with $\alpha = \gamma, Z$, we have, for massless electrons,

$$\frac{d\sigma_L}{d\Omega} \sim \sum_{\alpha,\beta} g_{Le}^\alpha g_{Le}^{\beta*} G^\alpha G^{\beta*} \times (W_1^{\alpha\beta} + \kappa_2 W_2^{\alpha\beta} \sin^2 \xi + \kappa_3 W_3^{\alpha\beta} \cos \xi), \quad (3.1)$$

$$\frac{d\sigma_R}{d\Omega} \sim \sum_{\alpha,\beta} g_{Re}^\alpha g_{Re}^{\beta*} G^\alpha G^{\beta*} \times (W_1^{\alpha\beta} + \kappa_2 W_2^{\alpha\beta} \sin^2 \xi - \kappa_3 W_3^{\alpha\beta} \cos \xi). \quad (3.2)$$

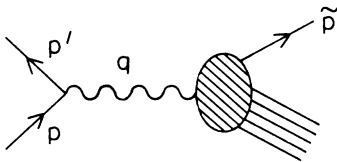


FIG. 3. $e^+e^- \rightarrow X + \text{anything}$ through one boson.

Here G^α are the photon and Z^0 propagators in lowest order in α_{em} :

$$G^\gamma = \frac{1}{q^2}, \quad G^Z = \frac{1}{q^2 + M_Z^2 - iM_Z \Gamma_Z} \quad (3.3)$$

and $\kappa_{2,3}$ are kinematical factors which do not depend on ξ , $\kappa_2 = |\vec{p}^2|/2$, $\kappa_3 = |\vec{p}|/\sqrt{s}$ with $s = -q^2$ in our metric. If we now integrate symmetrically in $\cos \xi$ from -1 to $+1$ the W_3 terms in $\sigma_{L,R}$ disappear. Then the longitudinal-polarization asymmetry is, after integrating over x for a massless final-state tagged hadron ($\vec{p}_0 = |\vec{p}|$),

$$A_{LR}(s) = \frac{\sum_{\alpha,\beta} (g_{Le}^\alpha g_{Le}^{\beta*} - g_{Re}^\alpha g_{Re}^{\beta*}) G^\alpha G^{\beta*} I^{\alpha\beta}}{\sum_{\alpha\beta} (g_{Le}^\alpha g_{Le}^{\beta*} + g_{Re}^\alpha g_{Re}^{\beta*}) G^\alpha G^{\beta*} I^{\alpha\beta}}, \quad (3.4)$$

where

$$I^{\alpha\beta} = \int_0^1 dx x \left[W_1^{\alpha\beta} + \frac{sx^2}{12} W_2^{\alpha\beta} \right]. \quad (3.5)$$

Note that since we integrated from -1 to $+1$ and over all tagged-hadron energies x , $I^{\alpha\beta}$ contains of course exactly the combination of structure functions appearing in the *total* cross section.

In perturbative QCD of *massless* quarks the α_s corrections can then be included as

$$I^{\alpha\beta}(q^2) = I^{\alpha\beta} |_{\alpha_s=0} \left[1 + \frac{\alpha_s(q^2)}{\pi} + O(\alpha_s^2) \right]. \quad (3.6)$$

Thus, the dependence of strong interaction would cancel through order α_s in $A_{LR}^{e^+e^- \rightarrow \text{hadrons}}$ for *light* hadrons in *total cross sections even off resonance*. [For top-quark production, this argument is no longer valid. Also the assumption of masslessness for, say, b quarks is suspect. A more detailed discussion of the cancellation of $O(\alpha_s)$ contribution to A_{LR} is given in the Appendix, along with some warning as to possible difficulties.]

Before moving on to the $O(\alpha_{em})$ corrections we note the following important property of A_{LR} . Although away from resonance it is final-state flavor dependent (and strong-interaction independent), it is a smooth function of \sqrt{s} which depends very weakly on \sqrt{s} near the pole. This is illustrated in Fig. 4 where we display A_{LR} , calculated with the computer program BREMMUS discussed in the next section, for various final states. These properties will be very useful when discussing the effects of initial-state bremsstrahlung in the next section.

IV. $O(\alpha_{em})$ CORRECTIONS TO A_{LR}

We now turn to the issue of $O(\alpha_{em})$ corrections to A_{LR} . These are of several types and we deal with each class separately below. The first class is the so-called "oblique" corrections depicted in Fig. 5. The shaded ovals are the renormalized one-particle-irreducible (1PI) vector self-energies. As has been shown,¹ these have the effect of renormalizing the coupling constants of photons and Z^0 's to fermions in $e^+e^- \rightarrow ff$, $(g_{L,R}^Z)_e, (g_{L,R}^Z)_f, (g_{L,R}^Z)_f$, making them functions of $q^2 = -s$. Imagine first that only Z^0 exchange occurred. Then according to Eq. (2.8) the dependence on $(g_{L,R}^Z)_f$ would cancel in

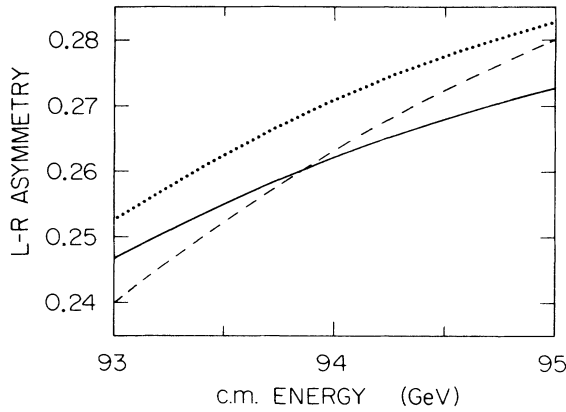


FIG. 4. $A_{LR}^{e^+e^- \rightarrow f\bar{f}}$ for $f = \mu$ (solid line), $f = u$ (dashed), and $f = d$ (dotted) neglecting final-state strong interactions as calculated by BREMMUS with $M_Z = 94$ GeV. Taken from entry (ii) in Table I.

$A_{LR}^{e^+e^- \rightarrow \text{hadrons}}$ and the dependence on $(g_{L,R}^Z)_e$ would be exactly the same as in $A_{LR}^{e^+e^- \rightarrow \mu^+\mu^-}$. Thus the important information about one-loop effects in GSW and beyond^{1,3} in the eZ coupling would be preserved in $A_{LR}^{e^+e^- \rightarrow f\bar{f}}$. The only problem is that there is also photon exchange, but the effects of the renormalization of $(g_{L,R}^Z)_e$ and $(g_{L,R}^Z)_f$

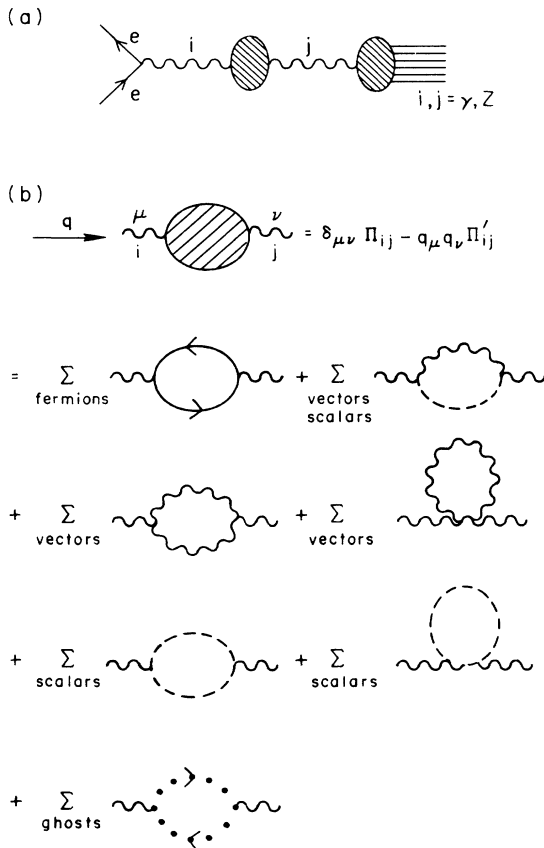


FIG. 5. Oblique corrections to $e^+e^- \rightarrow \text{hadrons}$.

would be first felt at the Z^0 pole at $O((\alpha/\pi)\Gamma_Z^2/M_Z^2)$ if all such corrections were real and at $O((\alpha/\pi)\Gamma_Z/M_Z)$ if the oblique corrections had imaginary parts as well. This is, at worst, an effect of $\sim 10^{-4}$ and so must be negligible. Thus at Z^0 pole $A_{LR}^{e^+e^- \rightarrow f\bar{f}} = A_{LR}^{e^+e^- \rightarrow \mu^+\mu^-}$ including oblique corrections in both the left-hand side (LHS) and right-hand side (RHS) and hadronization in the RHS as well. The next set of corrections are the so-called “direct” corrections to the electron vertices depicted in Fig. 6. The shaded blob depicts the 1PI $O(\alpha_{em})$ corrections to the Z and γ coupling to electrons. These again have only the effect of renormalizing these couplings making them functions of s , and so the argument given above holds as does Eq. (2.8). The next set of corrections is depicted in Fig. 7. Again, these only renormalize $(g_{L,R})_f$ and the usual argument applies on Z^0 pole as does Eq. (2.8). We might worry though about those corrections having to do with hadrons rather than quarks as in Fig. 8. But such graphs would only give $O(\alpha_{em})$ corrections to the Z^0 total decay rate when the final-state hadrons are integrated over a 4π detector, and this cancels in $A_{LR}^{e^+e^- \rightarrow \text{hadrons}}$ as argued in Eq. (2.8). They would reappear in the photon-exchange graphs, but as argued above would again only contribute negligibly to $O((\alpha/\pi)\Gamma_Z/M_Z)$ at worst. The last of the purely weak corrections have the structure of boxes as in Fig. 9. These cannot have a Z^0 pole structure (on Z^0 resonance we do not have enough energy to create two Z^0 s or two W s) at $q^2 = -M_Z^2$ and so contribute negligibly. Note that in order to avoid suppression factors of $G_\mu m_{\text{hadron}}^2 \sim 10^{-5}$ the virtual momentum k in the loops in Figs. 6–9 must be order $k \sim M_Z$. Thus the contributions of the graphs in Figs. 8 and 9 can be evaluated with perturbative QCD and have negligible strong-interaction uncertainty.

We now turn to QED corrections, the most dangerous of all. The largest such corrections come from the infrared part of the QED vertices and initial-state soft-photon bremsstrahlung depicted in Fig. 10. The infrared part divergent in the photon mass λ in Fig. 10(a) (part of the “direct” corrections) is of course canceled by that in Fig. 10(b), leaving us with a large correction depending upon the experimental resolution ΔE as $\lambda \rightarrow 0$. After ex-

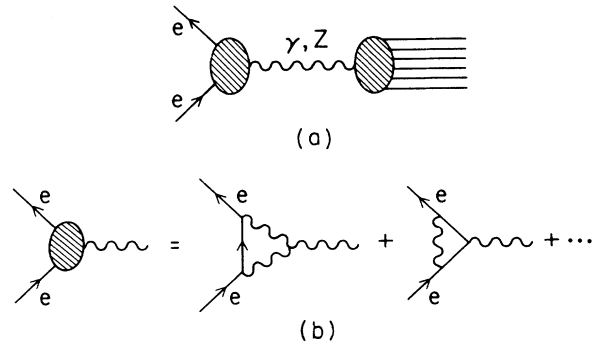


FIG. 6. Direct corrections to the electron vertices.

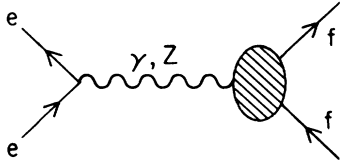


FIG. 7. Direct corrections to the $f\bar{f}$ vertex.

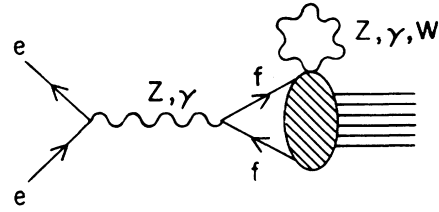


FIG. 8. Direct corrections to the final hadrons.

ponentiation (inclusion of many soft photons) this has the effect

$$\sigma_{L,R} \rightarrow \sigma_{L,R} \left[\frac{\Delta E}{E} \right]^{(2\alpha/\pi)(\ln s/m_e^2 - 1)} \quad (4.1)$$

with E the beam energy and experimental resolution $\Delta E \simeq 0.01E$. But this helicity-independent factor cancels in A_{LR} . The remaining contribution of Fig. 10(a) QED vertices gives an s -dependent renormalization of $(g_{L,R}^{\gamma})_e$ and $(g_{L,R}^Z)_e$ and the arguments given above still apply.

The remaining contributions from Fig. 10(b) are divided into two parts. The first set are soft photons or hard (detectable) almost beam collinear photons but in any case with $k \ll p, p'$. As is well known these mostly contribute to the classical radiation field after you add up enough of them [diagrams with more such independent initial-state bremsstrahlung photons than in Fig. 10(b)]. Thus we write

$$\begin{aligned} \sigma_L^{e^+e^- \rightarrow \bar{f}f + \text{photons}(s)} \\ = \sigma_L^{e^+e^- \rightarrow \bar{f}f}(s) + \frac{\alpha}{\pi} \int^s ds' P(s') \sigma_L^{e^+e^- \rightarrow \bar{f}f}(s'), \end{aligned} \quad (4.2)$$

where, for one-photon bremsstrahlung,

$$P(s') \sim \left[\frac{p}{p \cdot k} - \frac{p'}{p' \cdot k} \right]^2. \quad (4.3)$$

Here $s' = -(p - p' - k)^2$ and $(\alpha/\pi)P(s')$ is the probability of bremsstrahlung such that momentum s' flows through the virtual γ or Z^0 in Fig. 10(b). Similarly we write, for $k \ll p, p'$,

$$\begin{aligned} \sigma_R^{e^+e^- \rightarrow \bar{f}f + \text{photons}(s)} \\ = \sigma_R^{e^+e^- \rightarrow \bar{f}f}(s) + \frac{\alpha}{\pi} \int^s ds' P(s') \sigma_R^{e^+e^- \rightarrow \bar{f}f}(s), \end{aligned} \quad (4.4)$$

where the *same* helicity-independent function $P(s')$ appears in σ_R . A little manipulation yields, to $O(\alpha_{em})$,

$$\begin{aligned} A_{LR}^{e^+e^- \rightarrow \bar{f}f + \text{photons}(s)} \simeq A_{LR}(s) e^{e^+e^- \rightarrow \bar{f}f} + \frac{\alpha}{\pi} \int^s [A_{LR}^{e^+e^- \rightarrow \bar{f}f}(s') - A_{LR}^{e^+e^- \rightarrow \bar{f}f}(s)] \\ \times \frac{\sigma_t^{e^+e^- \rightarrow \bar{f}f}(s')}{\sigma_t^{e^+e^- \rightarrow \bar{f}f}(s)} P(s') ds', \quad \sigma_t = \sigma_L + \sigma_R. \end{aligned} \quad (4.5)$$

We now note the following facts about the second term on the RHS: $A_{LR}^{e^+e^- \rightarrow \bar{f}f}(s)$ is not a steep function of s near Z^0 resonance as indicated in Fig. 4 and so the brackets are very small. Further, at $s = M_Z^2$, $\sigma_t(s')/\sigma_t(s) \leq 1$ because of the Z^0 peaking structure. Thus initial-state soft radiation is negligible for A_{LR} . Note that $A_{FB}^{e^+e^- \rightarrow \mu^+\mu^-}$ is a *very* steep function of s near Z^0 resonance, and so there will be no such cancellation in that case. These comments are borne out by the direct calculations in 1982 of soft-photon QED corrections to various e^+e^- processes with polarized electrons by Bohm and Hollik.⁶ We defer discussion of hard photon $k \simeq p, p'$ effect from Fig.

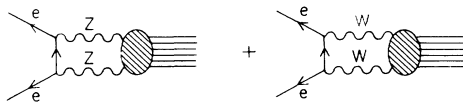


FIG. 9. Purely electroweak boxes.

10(b) until later.

The next set of graphs to be considered, shown in Fig. 11, integrates symmetrically to zero in $\cos\theta$ because of the G -parity conjugation properties of the photon. Now con-

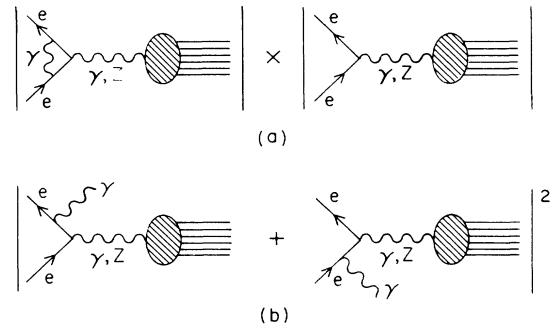


FIG. 10. Interference of QED vertices and initial-state bremsstrahlung.

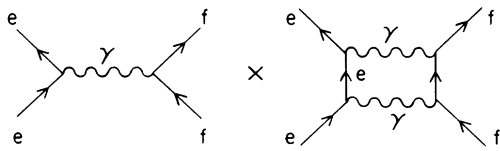


FIG. 11. Interference of γ - γ boxes with tree-level photon exchange.

sider the interference terms between initial- and final-state bremsstrahlung in Fig. 12. These are again divided into two groups. The first group is soft photons or hard collinear with $k \ll p, p'$. These can be written as proportional to

$$\left[\frac{p'}{p' \cdot k} - \frac{p}{p \cdot k} \right] \cdot \left[\frac{q_+}{q_+ \cdot k} - \frac{q_-}{q_- \cdot k} \right], \quad (4.6)$$

where q_{\mp} are the momenta of f and \bar{f} . Under ($\cos\theta \rightarrow -\cos\theta$), $q_+ \leftrightarrow q_-$ and the soft parts of the graphs in Fig. 12 also integrate symmetrically in $\cos\theta$ to zero. One may worry about the exponentiation factor of the infrared part $\sim \ln\lambda$ (with λ the photon mass) which comes from many such final-state photons' interference with initial-state photons. After cancellation of the IR parts with the IR parts of QED box graphs with at least one γ to be discussed later, a large factor

$$\left[\frac{\Delta E}{E} \right]^{-(4\alpha/\pi)Q_f^2 \ln[(1-\cos\theta)/(1+\cos\theta)]} \quad (4.7)$$

emerges. But this is helicity independent and factorizes out of A_{LR} . We defer discussion of hard bremsstrahlung photons $k \simeq p, p'$ in Fig. 12 until later.

We now turn to final-state radiation and QED corrections to final-state vertices as in Fig. 13. The graphs of Fig. 13(a) (also included in the "direct" corrections) simply renormalize $(g_{L,R}^{\gamma,Z})_f$ and so can be neglected according to our previous arguments. The infrared-divergent part of course is controlled by the IR-divergent part of the graphs of Fig. 13(b) resulting in a helicity-independent factor

$$\left[\frac{\Delta E}{E} \right]^{(2\alpha/\pi)Q_f^2(\ln s/m_f^2 - 1)} \quad (4.8)$$

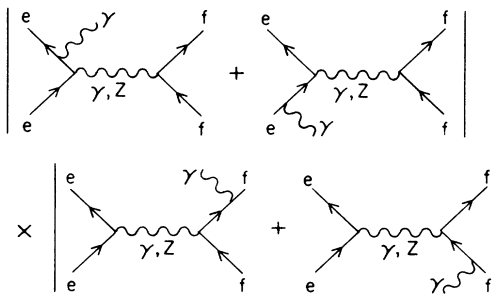
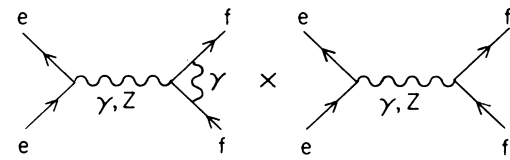
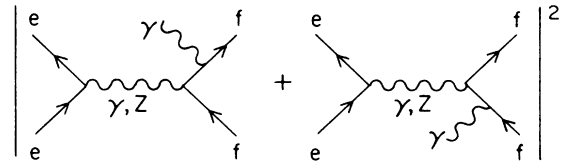


FIG. 12. Interference of initial- and final-state bremsstrahlung.



(a)



(b)

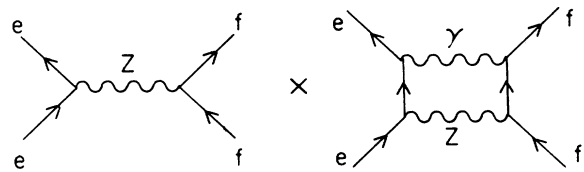
FIG. 13. Final-state radiation and QED corrections to final-state vertices.

which is simply absorbed in $(g_{L,R}^{\gamma,Z})_f$ and thus does not contribute to A_{LR} on Z^0 resonance. The soft photons or hard collinear photons with $k \ll p, p'$ in Fig. 13(b) which result in a factor

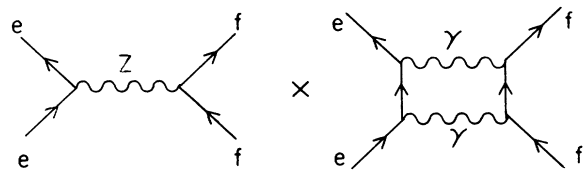
$$\left[\frac{q_+}{q_+ \cdot k} - \frac{q_-}{q_- \cdot k} \right]^2, \quad (4.9)$$

do not integrate symmetrically to zero, but may be absorbed in the coupling constants $(g_{L,R}^{\gamma,Z})_f$ when integrated over a 4π detector.

It is now time to turn to the γ - Z boxes of Fig. 14. We



(a)



(b)

FIG. 14. γ - Z boxes.

have already noticed that the IR-divergent part as $\lambda \rightarrow 0$ integrates symmetrically to zero for the one-loop graph; even after exponentiation the factor $\int (\Delta E/E)$ in Eq. (4.7) can be absorbed into a coupling constant. The contributions in Fig. 14(b) do not have a double pole on Z^0 resonance, but they do have large logarithms. The contributions of Fig. 14(a) have both a double pole and large logarithms, and are therefore the most dangerous. They have been calculated by Bohm and Hollik⁶ as well as by Brown, Decker, and Paschos⁷ and so, neglecting strong interactions, they are known functions which can be numerically computed. We note that the contributions of Fig. 14, especially 14(a), do *not* factorize and therefore, in principle, they bring quark-flavor dependence as well as strong-interaction dependence to $A_{LR}^{e^+e^- \rightarrow \text{hadrons}}$ even on Z^0 resonance. We are worried in particular by the hadronization of the final-state quarks in Fig. 14(a), as depicted in Fig. 15. In fact, the $|q^2|$ running through the Z^0 line must remain large to get the Z^0 pole enhancement and therefore the Z^0 couples primarily to a free quark line and we probably are able to use perturbative QCD in those parts of the graph. The photon, then, must be soft. Thus, perturbative arguments cannot be used in the evaluation of its coupling to hadrons so that some specific model of hadrons must probably be used; a soft long-wavelength photon will couple to the electric charge of a pion, nucleon, or other hadron rather than to the electric charge of their constituent partons. We have evaluated the graph of Fig. 14(a) numerically for free quarks and found its contribution to $A_{LR}^{e^+e^- \rightarrow f\bar{f}}$ to be small in agreement with Bohm and Hollik.⁶ Certainly, the graphs of Fig. 14(a) and the strong-interaction effects in Fig. 15 deserve further attention.

We continue our discussion of the $O(\alpha_{em})$ corrections with a comment about hard photons $k \simeq p, p'$ in Figs. 13(b), 12, and 10(b). These also do not factorize and may give rise to flavor dependence and strong-interaction dependence in $A_{LR}^{e^+e^- \rightarrow \text{hadrons}}$ even on Z^0 resonance. The photon cannot be too energetic, however, for then we would lose the Z^0 pole enhancement. Such effects are also deserving of further study. We will give below the results of the numerical calculation of these nonfactorizing graphs in order to estimate the associated strong-interaction uncertainties.

So far all of our remarks have been qualitative in nature. We now turn to quantitative results⁸ for the longitudinal-polarization asymmetry for $e^+e^- \rightarrow f\bar{f}(\gamma)$, where $f = u, d, \mu$ and either zero or one photon is included in the final state. These have been computed⁹ through $O(\alpha_{em})$ including *all* effects¹⁰ in the GSW $SU(2)_L \times U(1)$

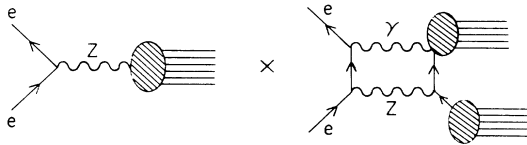


FIG. 15. An example of corrections coming from hadronization of the final-state quarks which may give a non-negligible strong-interaction uncertainty.

model, i.e., all “oblique” and “direct” electroweak radiative corrections as well as boxes and QED corrections with vertices and both soft and hard bremsstrahlung of *either zero or one photon*. The first calculation of electroweak GSW radiative corrections to $A_{LR}^{e^+e^- \rightarrow f\bar{f}}$ was by Lynn and Stuart,⁹ it was first stated there that the longitudinal-polarization asymmetry on Z^0 resonance including Born terms and “oblique” and other $O(\alpha_{em})$ weak corrections was almost independent of final-state flavor and that the leading perturbative QCD corrections canceled. $A_{LR}(-M_Z^2)$ was first shown independent of *soft* bremsstrahlung and QED vertices by Bohm and Hollik.⁶ The amplitudes for hard-photon bremsstrahlung with polarized beams were first written down by Kleiss.⁹

The Monte Carlo generator BREMMUS was written so that the various experimental cuts could be directly implemented. At the time of this writing, it is the *only* complete $O(\alpha_{em}^3)$ electroweak Monte Carlo program for e^+e^- polarized $\rightarrow f\bar{f}(\gamma)$. It includes some higher $O(\alpha_{em}^4)$ effects as well and will be discussed thoroughly elsewhere.⁸ BREMMUS allows us to compare directly theoretical and experimental results including the detector-dependent experimental cuts. It contains QCD strong-interaction effects *only* in vector-boson vacuum-polarization graphs; no attempt has been made to include by either perturbative QCD or hadronization models the strong interactions of final-state quarks.

The numerical results for $A_{LR}^{e^+e^- \rightarrow f\bar{f}(\gamma)}$ with $f = u, d, \mu$ are given in Table I. There we have taken $M_Z = 94$ GeV, $m_{\text{top}} = 30$ GeV, $m_{\text{Higgs}} = 100$ GeV, and $m_e = 0$ (except in infrared logarithms) and $m_f = 0.1$ GeV. Dependence on the final-state fermion mass (kept in IR logarithms only) is negligible for $m_f < 5$ GeV. The results are displayed for three center-of-mass energies: $M_Z - 1$ GeV, M_Z , and $M_Z + 1$ GeV. We take $A_{LR}^{e^+e^- \rightarrow \text{hadrons}}$ as given by $e^+e^- \rightarrow 2\bar{u}u(\gamma) + 3\bar{d}d(\gamma)$ meant to mimic *udscb* quarks.

Events generated were integrated over a 4π detector and the beam polarization was taken to be $P = 100\%$. 100 000 events were generated in each run. In addition the angle between f or \bar{f} and the beam lines was required to be greater than 20° and both f and \bar{f} were required to carry ≥ 15 GeV energy. The maximum hard-photon energy was taken to be $0.9E_{\text{beam}}$ while the experimental resolution for the soft photons was taken to be $\Delta E = 0.01E_{\text{beam}}$. Three results are displayed for each energy. If ξ_{acol} is the acollinearity cut angle between f and \bar{f} , we have displayed the results when the following hold.

- (i) Generated events were cut if $\xi_{\text{acol}} > 2^\circ$.
- (ii) No acollinearity cut was made.

(iii) The asymmetry is calculated *dropping only final-state fermion radiation to real and virtual photons in relative $O(\alpha_{em})$ graphs*. In other words, the dangerous contributions depicted in Figs. 11, 12, 13(a), 13(b), 14(a), and 14(b) have been set to zero in BREMMUS here. Note that the lowest order photon-exchange diagram squared in Fig. 16 as well as the initial-state radiation in Fig. 10 are still included in the numerical calculation. No acollinearity cut was made.

We now discuss the results of the numerical calculations. Note from comparison of the results with and without the acollinearity cut [entries (i) and (ii)] that the

TABLE I. Numerical results for $A_{LR}^{e^+e^- \rightarrow f\bar{f}(\gamma)}$ with polarization $P = 100\%$ with up to one photon in the final state calculated to $O(\alpha_{em})$ in GSW including *all* one-loop electroweak effects. Entries are (i) events with $\xi_{acoll} > 2^\circ$ cut, (ii) no acollinearity cut, and (iii) excluding the contributions of Figs. 11–14. Figures 16 and 10 are still included and no acollinearity cut has been made in (iii). Final-state strong-interaction effects are neglected throughout. Here $M_Z = 94$ GeV, $m_t = 30$ GeV, and $M_{\text{Higgs}} = 100$ GeV.

	\sqrt{s}	$\bar{u}u$	$\bar{d}d$	$2\bar{u}u + 3\bar{d}d$	$\mu^+\mu^-$
(i) $\xi_{acoll} \leq 2^\circ$	$M_Z + 1$ GeV	0.2838	0.2855	0.2849	0.2766
	M_Z	0.2640	0.2737	0.2705	0.2659
	$M_Z - 1$ GeV	0.2399	0.2572	0.2514	0.2525
(ii) No cut in acollinearity	$M_Z + 1$ GeV	0.2802	0.2827	0.2819	0.2728
	M_Z	0.2632	0.2710	0.2683	0.2622
	$M_Z - 1$ GeV	0.2400	0.2526	0.2482	0.2468
(iii) No final-state photon radiation	$M_Z + 1$ GeV	0.2823	0.2808	0.2814	0.2733
	M_Z	0.2642	0.2699	0.2679	0.2599
	$M_Z - 1$ GeV	0.2375	0.2521	0.2471	0.2468

effect of hard and soft bremsstrahlung is very small for a given flavor. There are still some flavor-dependent effects on pole but these can be traced to the graph with pure photon exchange in Figs. 16 and 10 as can be seen from comparison with entry (iii) which neglects the final-state fermion radiation to real (soft and hard) and virtual photons in relative $O(\alpha_{em})$ graphs only. As shown above, however, the flavor-dependent effects of the pure photon exchange graph in Figs. 16 and 10 can be included by calculation using perturbative QCD and thus the largest fraction of flavor-dependent effects give negligible strong-interaction uncertainty.

As mentioned above, the computer program BREMMUS contains no final-state strong-interaction effects. We will assume, however, that final-state strong-interaction effects can be no larger than flavor-dependent effects calculated in the absence of final-state hadronization. We thus take as an upper bound on strong-interaction uncertainties in $A_{LR}^{e^+e^- \rightarrow \text{hadrons}}$ the results given by BREMMUS for the various flavor-dependent contributions which cannot be calculated in perturbative QCD; in other words, we ascribe a 100% uncertainty to these contributions. These include γ - Z boxes and hard-photon effects [as well as other effects dropped in entry (iii) in Table I] as discussed above but not the contribution of Figs. 16 and 10. We estimate the theoretical strong-interaction uncertainty

$$\Delta A_{LR}^{e^+e^- \rightarrow \text{hadrons}}(-M_Z^2) \lesssim \pm 0.0005 \pm 0.0035, \quad (4.10)$$

where the first error is inferred from Table I [by the difference between entries (ii) and (iii) in the column with

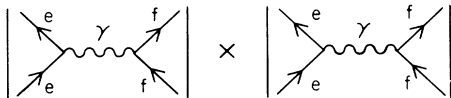


FIG. 16. Squared photon-exchange graph still included in A_{LR} in entry (iii) in Table I. This gives the vast majority of flavor-dependent effects.

final state $2\bar{u}u + 3\bar{d}d$, meant to give the asymmetry with final state $udscb$ quarks] and the second is from the strong-interaction uncertainty in the vector-boson vacuum polarization.¹¹ Note that (by these rules) even off resonance by ± 1 GeV, we can ascribe a small-strong-interaction uncertainty $\lesssim \pm 0.001 \pm 0.0035$.

Equation (4.10) is the main result of this section. We believe it gives a conservative estimate of the total theoretical error from strong-interaction uncertainties. We conjecture that more sophisticated calculations (higher order in perturbative QCD, specific hadronization models, inclusion of more soft and hard photons in the initial and final state, etc.) will further vindicate this estimate of the total strong-interaction theoretical error of $\lesssim \pm 0.004$, roughly 1.5% of $A_{LR}(-M_Z^2)$ itself. This must then be the experimental error design goal.

Note that the strong-interaction uncertainty in $A_{LR}^{e^+e^- \rightarrow \text{hadrons}}$ is not really any worse than that in $A_{LR}^{e^+e^- \rightarrow \mu^+\mu^-}$. It has been shown¹¹ that the strong-interaction uncertainty in $A_{LR}^{e^+e^- \rightarrow \mu^+\mu^-}$ is ± 0.0035 and, as stressed first in Ref. 11, is mainly due to the *quoted* experimental uncertainties in $e^+e^- \rightarrow \text{hadrons}$ in the region $1 \leq \sqrt{s} \leq 10$ GeV. This could be improved to $\sim \pm 0.0015$ if the experimental error in this region could be reduced to $\pm 5\%$ in the value of R . This would then bring the total theoretical strong-interaction error in $A_{LR}^{e^+e^- \rightarrow \text{hadrons}}$ to ± 0.002 . Such measurements on $e^+e^- \rightarrow \text{hadrons}$ between 1 and 10 GeV should thus be given high priority so that SLC/LEP can give a very-high-precision test of electroweak theory.

V. MEASUREMENT OF A_{LR} AND CONCLUSIONS

Having finished our discussion of the longitudinal-polarization asymmetry $A_{LR}^{e^+e^- \rightarrow \text{hadrons}}$ near Z^0 resonance, we now turn to the experimental implications of this asymmetry for testing GSW at the one-loop level as well as the possibility of theories beyond GSW.

Table II contains the shifts $\Delta A_{LR}^{e^+e^- \rightarrow \mu^+\mu^-}(-M_Z^2)$ in the longitudinal-polarization asymmetry for various

TABLE II. Response of one-loop various asymmetries on Z_0 resonance to new one-loop physics (taken from Refs. 1 and 3). Results listed are only representative of these *model-dependent* effects.

One-loop physics	$\delta A_{LR} = \delta A_{rpol}$	$\delta A_{FB}^{e^+e^- \rightarrow \mu^+\mu^-}$	δM_W (MeV)
Photon vacuum polarization	-0.12	-0.06	-890
GSW weak $m_t = 30$ $m_H = 100$	-0.03	-0.01	-180
Heavy top quark $m_t \simeq 180$ GeV	0.03	0.0075	780
Heavy Higgs boson ~ 1 TeV	-0.01	-0.0045	-160
Heavy-quark pair (a) Large I splitting (b) Degenerate	0.02 -0.004	0.01 -0.002	300 -42
Heavy-lepton pair (a) Large I splitting $m_\nu = 0$ (b) Degenerate	0.012 -0.0013	0.006 -0.0006	300 -14
Heavy-scalar-quark pair (a) Large I splitting (b) Degenerate	0.02 0	0.01 0	300 0
Heavy-scalar-lepton pair (a) Large I splitting (b) Degenerate	0.012 0	0.006 0	300 0
Technicolor SU(8) \times SU(8) O(16)	-0.04 -0.07	-0.018 -0.032	-500 -500
SU(2) _L \times U(1) _Y \times U(1) _{Y'} $M_{Z'}/M_Z = 3$	-0.03	-0.01	+2500
SU(2) _L \times SU(2) _R \times U(1) _{B-L} $M_{Z'}/M_Z = 5$	0.08	0.03	1500

sources of interesting and new physics. These are mostly due to ‘‘oblique’’ radiative corrections¹ or to the effect of new gauge particles in extended gauge groups³ at the tree level and so are the same as the shifts in $A_{LR}^{e^+e^- \rightarrow \text{hadrons}}$ as shown in Refs. 1 and 3:

$$\delta A_{LR}^{e^+e^- \rightarrow \mu^+\mu^-}(-M_Z^2) = \delta A_{LR}^{e^+e^- \rightarrow \text{hadrons}}(-M_Z^2). \quad (5.1)$$

These then are typically of order 1% although they can be much larger; the goal must then be to measure experimentally and interpret theoretically $A_{LR}^{e^+e^- \rightarrow \text{hadrons}}$ to $\lesssim \pm 0.005$. Note that the forward-backward asymmetry $A_{FB}^{e^+e^- \rightarrow \mu^+\mu^-}(-M_Z^2)$ is much less sensitive to this interesting physics. We compare the shifts in the asymmetries with the shift in the W^\pm mass δM_W in Table II.

A detailed study of experimental errors, etc., can be found in the formal proposal for e^- beam polarization of the SLC polarization group SLCPOL¹² and much of what follows is drawn from there. The main source of systematic experimental error for A_{LR} is the uncertainty ΔP in the value of the absolute e^- beam polarization P .

These we take to be $P \simeq 40\%$ and $\Delta P/P = \pm 0.05$, values already achieved at SLAC in 1978 for the polarized electron-deuteron experiment. Note, however, that the longitudinal-polarization asymmetry is quite insensitive to this systematic error; an experimental error

$$\Delta A_{LR} \simeq \frac{\Delta P}{P} A_{LR} \simeq 0.27 \frac{\Delta P}{P} \quad (5.2)$$

is induced in A_{LR} for $M_Z = 94$ GeV. There is a statistical experimental error which depends on the beam luminosity or the number of Z^0 's produced in e^+e^- annihilation. Further we take the theoretical error in $A_{LR}^{e^+e^- \rightarrow \text{hadrons}}$ to be ± 0.004 and in $A_{LR}^{e^+e^- \rightarrow \mu^+\mu^-}$ to be ± 0.0035 .

In Fig. 17(a) (RHS, solid line) the *total* experimental plus theoretical uncertainty in $A_{LR}^{e^+e^- \rightarrow \mu^+\mu^-}(-M_Z^2)$ is plotted as a function of the beam luminosity for $\Delta P/P = \pm 0.05$, $P = 40\%$. Note that we need approximately 10^6 Z^0 's to test $A_{LR}^{e^+e^- \rightarrow \mu^+\mu^-}(-M_Z^2)$ to $\sim \pm 0.02$ because the error is statistics dominated even then. We have indicated in this paper, however, that we are able to

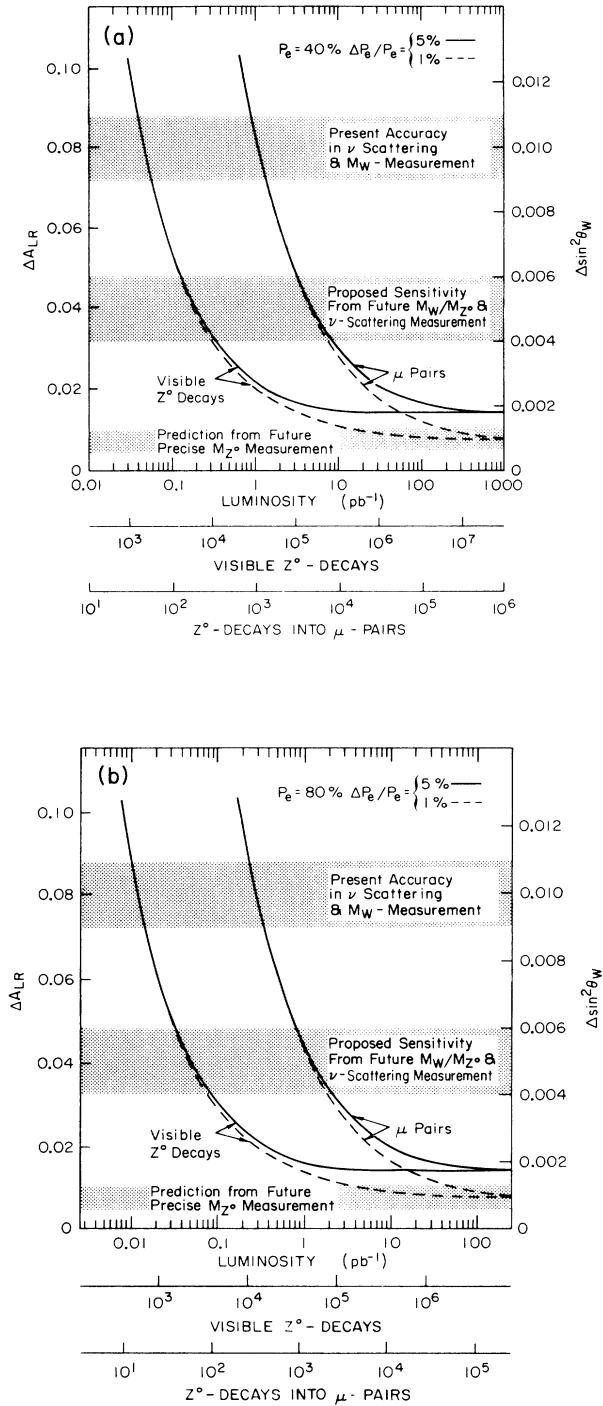


FIG. 17. (a) Total experimental and theoretical uncertainty in $A_{LR}^{e^+e^- \rightarrow \mu^+\mu^-}(-M_Z^2)$ (RHS lines) and $A_{LR}^{e^+e^- \rightarrow \text{hadrons}}(-M_Z^2)$ (LHS lines) as a function of the beam luminosity assuming $\Delta P/P = \pm 0.05$, $P = 40\%$ (solid lines) and $\Delta P/P = \pm 0.01$, $P = 40\%$ (dashed lines). A theoretical strong-interaction uncertainty of ± 0.004 for $A_{LR}^{e^+e^- \rightarrow \text{hadrons}}(-M_Z^2)$ has been assumed. It has been shown (Ref. 10) that the strong-interaction uncertainty in $A_{LR}^{e^+e^- \rightarrow \mu^+\mu^-}(-M_Z^2)$ is ± 0.0035 . Also indicated is the resultant total experimental plus theoretical uncertainty in $\sin^2\theta_W$. (b) The same as (a) but with polarization $P = 80\%$.

reduce the total theoretical strong-interaction uncertainty in $A_{LR}^{e^+e^- \rightarrow \text{hadrons}}(-M_Z^2)$ to $\lesssim \pm 0.004$. In Fig. 17(a) (LHS, solid line) the resulting *total* experimental plus theoretical error in $A_{LR}^{e^+e^- \rightarrow \text{hadrons}}(-M_Z^2)$ is plotted as a function of the beam luminosity. With only $\sim 5 \times 10^4$ Z^0 's (early in SLC lifetime) the asymmetry can be measured to ± 0.015 which could be regarded as a measure of $\sin^2\theta_W$ to ± 0.002 giving already a very serious constraint on the physics of Table II. Note that $A_{LR}^{e^+e^- \rightarrow \text{hadrons}}$ is not statistics dominated after $\sim 10^6$ Z^0 's; we need then to bring down the systematic error.

It may be possible to improve the e^- beam polarization to $P \approx 100\%$ using stressed uniaxial crystals¹² and separately to improve the polarization measurement to $\Delta P/P = \pm 0.01$ with a Compton polarimeter.¹² In anticipation of these developments, the experimental and theoretical uncertainties in $A_{LR}^{e^+e^- \rightarrow \mu^+\mu^-}(-M_Z^2)$ (RHS, dashed line) and $A_{LR}^{e^+e^- \rightarrow \text{hadrons}}(-M_Z^2)$ (LHS, dashed line) are plotted in Fig. 17(a) as functions of beam luminosity for $P = 40\%$, $\Delta P/P = \pm 0.01$. Figure 17(b) is similar to Fig. 17(a) but now with polarization $P = 80\%$. Note the increases in sensitivity. This certainly justifies giving high priority to these polarization improvements. It will then be possible to measure $A_{LR}^{e^+e^- \rightarrow \text{hadrons}}$ to ± 0.008 ($\sin^2\theta_W$ to ± 0.001) with $\sim 10^6$ Z^0 's.

We now compare the sensitivity to new and interesting physics of the longitudinal-polarization asymmetry $A_{LR}^{e^+e^- \rightarrow \text{hadrons}}$ with the forward-backward asymmetry $A_{FB}^{e^+e^- \rightarrow \mu^+\mu^-}$ on Z^0 resonance. In Fig. 18 these asymmetries are plotted as functions of M_Z in three cases: (i) without new physics (solid lines) $m_t = 30$, $m_{\text{Higgs}} = 100$ GeV; (ii) with a heavy top quark $m_t \approx 180$ GeV and

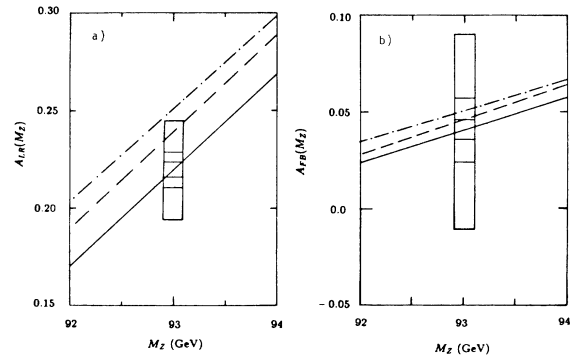


FIG. 18. (a) The left-right asymmetry evaluated at the Z as a function of the Z mass. The solid curve corresponds to $m_t = 30$ GeV, $M_H = 100$ GeV. The dotted-dashed curve corresponds to $m_t = 180$ GeV, $M_H = 100$ GeV. The dashed curve corresponds to $m_t = 30$ GeV and $M_H = 100$ GeV, but with $\rho = 1.01$ instead of $\rho = 1.00$. The rectangles indicate the expected limits for $\pm 1\sigma$ about a hypothetical data point on the solid curve with $M_Z = 93$ GeV with $P = 40\%$. The largest rectangle represents the expectation for $N = 10^4$ observed Z 's and $\Delta P/P = \pm 0.05$. The two smaller ones represent $N = 10^5$ with $\Delta P/P = \pm 0.03$ and $N = 10^6$ with $\Delta P/P = \pm 0.01$. (b) The forward-backward asymmetry for the $\mu^+\mu^-$ final state. The conventions are identical to those in (a).

$M_H = 100$ GeV (dotted-dashed lines); (iii) a shift in the asymmetries as would occur, for $M_t = 30$ GeV, $M_H = 100$ GeV (dotted lines), but now with a ρ parameter $\rho = 1.01$ from, say, the VEV of a Higgs triplet or a new representation of fermions with large custodial $SU(2)_L \times SU(2)_R$ symmetry breaking. These lines are *indicative* of the effects of new physics on the asymmetries and are not to be taken as precise predictions.

The rectangles in Figs. 18(a) and 18(b) indicate systematic and statistical experimental plus theoretical errors in the asymmetries with 10^4 , 10^5 , and 10^6 Z^0 's with increasingly smaller error bars. The boxes include a ± 50 MeV error on the direct experimental measurement of M_Z . Note that although A_{FB} is insensitive, A_{LR} can be used with relatively few Z^0 's to probe the effects of new and interesting physics at one loop in GSW, for new $SU(2)_L \times U(1)$ matter representations from beyond GSW and for new gauge sectors from beyond GSW.

We now turn to a comparison of the power of various precise measurements to constrain GSW at one loop as well as physics from beyond GSW. Imagine that all such experiments can be interpreted as measurements of M_Z . We plot in Fig. 19 the resulting experimental and theoretical uncertainties in M_Z from various experimental programs. To the left are "non-SLC/LEP" experiments including a direct measurement of M_Z by UA1 and UA2, neutrino-hadron scattering (the dotted part of the line indicates theoretical uncertainties beyond the quoted experimental ones) and neutrino-electron scattering as proposed for the 1990s by the CHARM II Collaboration. In the middle we plot SLC/LEP experiments without beam polarization with 10^4 , 10^5 , and 10^6 Z^0 's including a direct mass measurement and the forward-backward asymmetry $A_{FB}^{e^+e^- \rightarrow \mu^+\mu^-}$. On the right are plotted proposed

SLC/LEP experiments with 40% e^- beam polarization for 10^4 , 10^5 , and 10^6 Z^0 's. Note that $A_{LR}^{e^+e^- \rightarrow \text{hadrons}}$ with only $\sim 5 \times 10^4$ Z^0 's is already the best test of the theory and is bettered only by $A_{LR}^{e^+e^- \rightarrow \mu^+\mu^-}$ with about 10^7 Z^0 's because of its slightly smaller strong-interaction uncertainty.^{1,9,11}

ACKNOWLEDGMENTS

B.W.L. would like to thank the Department of Theoretical Physics of the University of Trieste and ISAS (Trieste) for their warm hospitality during his visit and the SLC polarization group¹² for interesting discussions. C.V. would also like to thank the Theoretical Physics Group at SLAC for warm hospitality. We are indebted to F. M. Renard and especially C. Y. Prescott for very illuminating discussions. We thank P. Grosse-Weismann for the use of his Figs. 17(a) and 17(b) and R. Cahn for the use of his Figs. 18 and 19. We are particularly appreciative of P. Rankin who found and fixed a programming error in the computer program BREMMUS and has subjected it to a terrible gauntlet of numerical tests. Further, she pointed out that we had been unnecessarily pessimistic in our initial severe overestimate of the theoretical error induced by strong-interaction effects in the final state because we had unnecessarily ascribed a 100% error to the *photon-exchange* graph with initial-state radiation in Fig. 10 which, of course, can be calculated in perturbative QCD.

APPENDIX

Consider the process $e^+e^- \rightarrow \bar{f}f$, where f is a certain quark, to lowest order in electroweak interactions but to all orders in the strong interactions. If $J_\mu^{\gamma,Z}$ are the hadronic components of the photon and Z^0 currents in the standard model and $|F\rangle$ denotes the final $|\bar{f}f\rangle$ state, we have

$$\langle 0 | J_\mu^i | F \rangle \langle F | J_\nu^j | 0 \rangle = S_{\mu\nu} F_S^{ij}(\bar{p}) + A_{\mu\nu} F_A^{ij}(\bar{p}), \quad i, j = \gamma, Z, \quad (A1)$$

where $S_{\mu\nu}, A_{\mu\nu}$ are kinematical coefficients which are symmetric and antisymmetric in the Lorentz indices and $F_{S,A}(\bar{p})$ contain the full effect of flavor and strong-interaction dependence of final states with a tagged hadron of momentum \bar{p} plus anything. When integrated symmetrically in $\cos\theta$, $\int F_A^{ij}$ vanishes and then as discussed in Ref. 5, one is led to an expression for the longitudinal-polarization asymmetry for the process $e^+e^- \rightarrow \bar{f}f$ with hadronization in terms of the symmetric parts F_S^{ij} . Note that, while $F_S^{\gamma\gamma}$ and F_S^{ZZ} are real, $F_S^{\gamma Z}$ in principle contains an imaginary part which must be taken into account.

Actually, $F_S^{\gamma Z}$ can only come from the interference of the photon current with the *vector* part of the Z^0 current. For the latter we write, following the decomposition used in Ref. 10,

$$J_{\text{vector}}^Z = - \left[\frac{\frac{1}{2} - s_\theta^2}{s_\theta c_\theta} J^\gamma + \frac{1}{s_\theta c_\theta} \Delta J \right], \quad (A2)$$

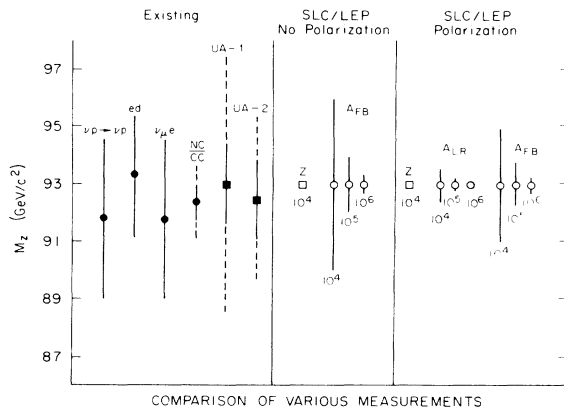


FIG. 19. Comparison of indirect measurements of the Z mass, assuming the standard electroweak model, with direct measurements. Squares indicate direct measurements; circles indirect measurements. The open circles and squares indicate future measurements; error bars show $\pm 1\sigma$. Existing data are taken from the 1986 Particle Data Group compilation. The asymmetry measurements at the SLC show three circumstances: $N = 10^4$, $\Delta P/P = 5\%$; $N = 10^5$, $\Delta P/P = 3\%$; $N = 10^6$, $\Delta P/P = 1\%$ all with $P = 40\%$.

where $s_\theta = \sin\theta_W$ is the weak mixing angle ($c_\theta^2 = 1 - s_\theta^2$) and

$$\begin{aligned} \Delta J &= J_{\text{vector}}^3 - \frac{1}{2} J^\gamma \\ &= \frac{1}{4} (J^{(\phi)} - 2J^{(\omega)}) + \Delta J^{(\text{heavy quarks})}, \end{aligned} \quad (\text{A3})$$

where $\Delta J^{(\text{heavy quarks})}$ contains the contributions from heavy (i.e., c, b, t, \dots) quarks. Note that the current for the vector ρ meson does not appear in Eq. (A3) while the currents $J^{(\phi)}$ and $J^{(\omega)}$ for the vector ϕ and ω do.

On Z^0 resonance, the interference between photon and Z exchange graphs can contribute if $F_S^{\gamma Z}$ develops an imaginary part. This can only come from *nondiagonal* (mixing) components, i.e., of the kind

$$\text{Im} \langle 0 | J_\mu^m | F \rangle \langle F | J_\nu^n | 0 \rangle, \quad (\text{A4})$$

where m, n ($m \neq n$) denote specific light (ρ, ω, ϕ) and/or heavy (c, b, t) components of the electromagnetic current. We can thus consider two different situations.

(1) f is a light (u, d, s) quark. Then, the ‘‘heavy’’ m, n indices are strongly suppressed by Zweig mechanisms. The light indices are suppressed, conversely, by ρ - ω , ω - ϕ , . . . mixing parameters. Roughly, we can classify the latter as being of either next order in α_{em} or proportional to light-quark mass differences which are absolutely negligible at the M_Z scale.

(2) f is a heavy (c, b, t, \dots) quark. Then, every index is

suppressed by Zweig mechanisms.

We thus conclude that $F_S^{\gamma\gamma}$, F_S^{ZZ} , and $F_S^{\gamma Z}$ are all real to high accuracy. If we now sum over all final states

$$\tilde{F}_S^{ij} = \sum_F \text{Re} \langle 0 | J^i | F \rangle \langle F | J^j | 0 \rangle \quad (\text{A5})$$

the \tilde{F}_S are directly related to the total cross sections for $e^+e^- \rightarrow \text{hadrons}$. In perturbative QCD we can use factorization theorems for the strong interactions of massless quarks and thus

$$\tilde{F}_S^{ij} = \tilde{F}_S^{ij} |_{\alpha_s=0} \left[1 + \frac{\alpha_s(\tilde{P})}{\pi} + O(\alpha_s^2(\tilde{P})) \right] \quad (\text{A6})$$

with $\tilde{F}_S^{ij} |_{\alpha_s=0}$ calculated in electroweak $SU(2)_L \times U(1)$ with QCD turned off.

Now consider the longitudinal-polarization asymmetry $A_{LR}^{e^+e^- \rightarrow \text{hadrons}}$. Since this is a *ratio* of total cross sections (with left- and right-handed electron beams) it depends on *ratios* of the \tilde{F}_S^{ij} and in such ratios strong-interaction effects *cancel* at least through $O(\alpha_s)$. These facts, not necessarily true for the antisymmetric parts or for the imaginary components of the hadronic tensors and, to our knowledge, for $(\bar{t}t)$ final states whose quark mass is comparable to M_Z , allow us to write near the Z^0 resonance ($f \neq e, \nu_e, t$):

$$A_{LR}^{e^+e^- \rightarrow f\bar{f}}(q^2) = A_{LR}^{e^+e^- \rightarrow f\bar{f}}(q^2) |_{\alpha_s=0} + O(\alpha_s^2). \quad (\text{A7})$$

- ¹B. W. Lynn, M. E. Peskin, and R. G. Stuart, in *Physics at LEP*, proceedings of the LEP Physics Jamboree, edited by J. Ellis and R. Peccei (CERN Report No. 86/02, 1986); for a recent review on this subject, see *Tests of Electroweak Theories*, proceedings of the Conference, Trieste, 1985, edited by B. W. Lynn and C. Verzegnassi (World Scientific, Singapore, 1986).
- ²S. L. Glashow, Nucl. Phys. **20**, 579 (1961); S. Weinberg, Phys. Rev. Lett. **19**, 1254 (1967); A. Salam, in *Elementary Particle Theory: Relativistic Groups and Analyticity*, edited by N. Svartholm (Nobel Symposium No. 8), (Amqvist and Wiksell, Stockholm, 1968), p. 367; S. L. Glashow, J. Iliopoulos, and L. Maiani, Phys. Rev. D **2**, 1285 (1970); G. 't Hooft, Nucl. Phys. **B33**, 173 (1971); **B35**, 167 (1971), and references therein.
- ³W. Hollik, Z. Phys. C **8**, 149 (1981); M. Cvetic and B. W. Lynn, Phys. Rev. D **35**, 51 (1987); P. J. Franzini and F. J. Gilman, *ibid.* **35**, 855 (1987). This last paper contains also a list of the most recent contributions to the subject.
- ⁴R. Kleiss, F. M. Renard, and C. Verzegnassi, Nucl. Phys. **B286**, 669 (1987); see also F. M. Renard and C. Verzegnassi, Phys. Lett. **B178**, 289 (1986).
- ⁵B. W. Lynn and C. Verzegnassi, Nuovo Cimento **94A**, 15 (1986).

- ⁶M. Bohm and W. Hollik, Nucl. Phys. **B204**, 45 (1982).
- ⁷R. W. Brown, R. Decker, and E. A. Paschos, Phys. Rev. Lett. **52**, 1192 (1984).
- ⁸D. Kennedy, R. Kleiss, B. W. Lynn, and R. G. Stuart, Report No. SLAC-PUB-4128, 1986 (unpublished).
- ⁹B. W. Lynn and R. G. Stuart, Nucl. Phys. **B253**, 216 (1985); R. Kleiss, Ph.D. thesis, University of Leiden, 1982; M. Bohm and W. Hollik (Ref. 6).
- ¹⁰Except those proportional to an external fermion mass $\sim m_e^2/q^2, m_f^2/q^2$ which are negligible for our purposes here but are not so for heavy top quarks in the final state.
- ¹¹B. W. Lynn, G. Penso and C. Verzegnassi, Phys. Rev. D **35**, 42 (1987).
- ¹²D. Blockus, J. M. Brom, H. Ogren, D. Rust, R. Cahn, O. Chamberlain, R. Fuzesy, G. Shapiro, H. Steiner, W. B. Atwood, J. Clendenin, D. Cords, T. Fieguth, P. Grosse-Wiesmann, L. Keller, B. W. Lynn, K. C. Moffeit, J. J. Murray, H. Petersen, C. Y. Prescott, C. Sinclair, S. St. Lorant, D. Walz, G. Diambri-Palazzi, M. Dameri, R. Parodi, R. Vaccarone, J. R. Johnson, T. Maruyama, and R. Prepost, SLAC reports, 1985 and 1986 (unpublished).